Quench-Flow Analysis Reveals Multiple Phases of GluT1-Mediated Sugar Transport†

David M. Blodgett and Anthony Carruthers*

Department of Biochemistry and Molecular Pharmacology, University of Massachusetts Medical School, 364 Plantation Street, Worcester, Massachusetts 01605

Received August 13, 2004; Revised Manuscript Received December 1, 2004

ABSTRACT: Standard models for carrier-mediated nonelectrolyte transport across cell membranes do not explain sugar uptake by human red blood cells. This means that either (1) the models for sugar transport are incorrect or (2) measurements of sugar transport are flawed. Most measurements of red cell sugar transport have been made over intervals of 10 s or greater, a range which may be too long to measure transport accurately. In the present study, we examine the time course of sugar uptake over intervals as short as 5 ms to periods as long as 8 h. Using conditions where transport by a uniform population of cells is expected to be monophasic (use of subsaturating concentrations of a nonmetabolizable but transported sugar, 3-*O*-methylglucose), our studies demonstrate that red cell sugar uptake is comprised of three sequential, protein-mediated events (rapid, fast, and slow). The rapid phase is more strongly temperature-dependent than the fast and slow phases. All three phases are inhibited by extracellular (maltose or phloretin) or intracellular (cytochalasin B) sugar-transport inhibitors. The rate constant for the rapid phase of uptake is independent of the 3-*O*-methylglucose concentration. The magnitude (moles of sugar associated with cells) of the rapid phase increases in a saturable manner with [3-*O*-methylglucose] and is similar to (1) the amount of sugar that is retained by red cell membrane proteins upon addition of cytochalasin B and phloretin and (2) the D-glucose inhibitable cytochalasin B binding capacity of red cell membranes. These results are consistent with the hypothesis that previous studies have both under- and overestimated the rate of erythrocyte sugar transport. These data support a transport mechanism in which newly bound sugars are transiently sequestered within the translocation pathway where they become inaccessible to extra- and intracellular water.

A family of glucose-transport proteins catalyzes the stereoselective, bidirectional, passive transport of sugar molecules across the cell membrane. One member of this family, human erythrocyte glucose transport protein (GluT1),[1] mediates sugar transport across the human erythrocyte membrane (*1*).

Although extensively studied, the molecular mechanism of GluT1-mediated sugar transport is unknown. In the absence of stable GluT1−substrate intermediates for structural analysis, researchers have used biochemical and biophysical approaches to investigate transport. Their results suggest three possible transport mechanisms. The transporter may function as a simple, alternating carrier, sequentially presenting sugar import (e2) and export (e1) sites (*2*−*5*). During uptake, extracellular sugar binding to the e2 site catalyzes a conformational change (e2 → e1) that releases bound sugar into cytosol and exposes an e1 site. The e2 confomer is regenerated for additional cycles of sugar import via the inverse (e1 → e2) conformational change resulting from either the binding and rapid export of intracellular sugar or from a slow, sugar-independent relaxation to the initial state. An alternative hypothesis describes a simultaneous-carrier mechanism, where the transporter molecule simultaneously exhibits import and export configurations (*6*−*8*). In this model, the transporter is proposed to be a complex of four GluT1 proteins in which each subunit (GluT1 protein) functions as a simple, alternating carrier. An obligate functional relationship between subunits is proposed to limit the conformational freedom of subunits within the transport complex. At any instant, therefore, two subunits must exist as e2 confomers, while the remaining two subunits must present e1 confomers (*9*). A third model suggests that GluT1-mediated sugar transport is inconsistent with the predictions of either of the preceding mechanisms. Imported sugars are proposed to interact with noncatalytic binding sites associated with the carrier or internal red cell components (*6*, *10*, *11*). This compromises the accuracy of transport determinations because intracellular $[sugar]_{total}$ > intracellular $[sugar]_{free}$.

The recent crystallization of lactose permease (LacY) in the e1 (export) configuration provides a clearer picture of a carrier substrate-binding site (*12*). Although not strictly a

† This work was supported by NIH Grant DK 44888.

* To whom correspondence should be addressed. E-mail: anthony.carruthers@umassmed.edu. Telephone: 508-856-5570. Fax: 508-856-6464.

[1] Abbreviations: GluT1, human erythrocyte glucose transport protein; 3MG, 3-*O*-methyl-α,D-glucopyranoside; C-Ab, rabbit polyclonal antiserum raised against a synthetic peptide comprised of GluT1 residues 480−492; CCB, cytochalasin B; CCD, cytochalasin D; EDTA, ethylenediaminetetraacetic acid; ELISA, enzyme-linked immunosorbent assay; HEPES, *N*-[2-hydroxyethyl]piperazine-*N*′-[2-ethanesulfonic acid]; HRP, horseradish peroxidase; RBC, red blood cell; SDS, sodium dodecyl sulfate; PAGE polyacrylamide gel electrophoresis; Tris-HCl, tris(hydroxymethyl)aminomethane hydrochloride.

10.1021/bi048247m CCC: $30.25
Published on Web 01/28/2005

passive sugar carrier, this proton−disaccharide symporter is capable of passive transport in the absence of an electrochemical gradient for proton-driven sugar transport (*13*). LacY is also a member of the wider major facilitator superfamily (MFS) of transporters, which includes the GluT family of carriers (*14*, *15*). The LacY e1 crystal structure is characterized by a large internal hydrophilic cavity (25 by 15 Å) extending from the cytosol to deep within the core of the membrane-embedded portion of the carrier. The volume of the cavity is approximately 1.5×10^{-24} L, a space large enough to contain as many as 3−5 hydrated glucose molecules assuming a self-diffusion coefficient of glucose of 4×10^{-6} cm^2 s^{-1} at 20 °C (*16*). It is proposed that, following substrate binding to e1, the cavity closes to engulf the bound sugar molecule and then opens at the opposite or trans side of the membrane to form a similar outward facing cavity into which the bound substrate can dissociate and subsequently diffuse into the interstitium (*12*). The e1 structure of a second MFS transporter, the bacterial glycerol-3-phosphate/P_i antiporter (GlpT), provides additional support for the alternating confomer transport mechanism in prokaryotes (*17*, *18*). The process by which the substrate-binding event promotes conformational changes that result in substrate translocation is unknown (*12*, *17*, *18*), and e2 or intermediate forms of LacY and GlpT are unavailable for more detailed analysis.

While the alternating confomer model for carrier-mediated transport gains strong support from the LacY and GlpT structures, it is also evident that this model does not quantitatively describe the sugar-transport properties of human red blood cells (RBCs) (*19*, *20*). Transport measurements obtained by conventional benchtop procedures indicate that the Haldane requirements for a passive transport mechanism ($V_{max}/K_{m(app)}$ ratios for exchange and net entry and exit of sugars must be equal) are not satisfied (*19*−*22*). More rapid sampling procedures (resolution < 1 s) obtained by quench flow (*5*) appear to result in transport parameters that satisfy the Haldane requirements. This suggests that red cell sugar transport is very fast and requires rapid sampling procedures for accurate determination of initial rates. However, these more rigorously determined Michaelis and velocity parameters fail to predict the kinetics of red cell sugar transport over physiological time intervals [from seconds to minutes (*19*, *20*, *23*−*25*)].

The present study was conducted to examine the kinetics of sugar uptake by human red cells over intervals ranging from milliseconds to hours. To achieve this, we used a rapid quench-flow device (which provides subsecond temporal resolution) in conjunction with reduced reaction temperature to study the earliest events associated with glucose transport. These studies provide evidence for at least three phases of protein-mediated glucose translocation into the red cell, provide "V_{max} and K_m" parameters for transport obtained during each of these phases, and suggest that it is possible to isolate an intermediate GluT1 form [e(S)] that bridges the eS2 → eS1 transition.

MATERIALS AND METHODS

Materials. [^{3}H]-3-*O*-Methylglucose ([^{3}H]-3MG) and [^{3}H]-cytochalasin B were purchased from Amersham Biosciences (Piscataway, NJ), and [^{3}H]-L-glucose was purchased from Sigma−Aldrich (St. Louis, MO). Rabbit antisera against amino acid residues 480−492 of the GluT1 carboxy terminus (C-Ab) were prepared as described in ref *26* and obtained from Animal Pharm Services, Inc. (Healdsburg, CA). Goat anti-rabbit (GAR) horseradish peroxidase (HRP) conjugate was purchased from Bio-Rad Laboratories (Hercules, CA). Washed RBCs and whole blood stored in CPDII AS-1 preservative solution were obtained from Biological Specialties Corporation (Colmar, PA). All other reagents were purchased from Sigma−Aldrich unless otherwise noted.

Solutions. KCl saline (kaline) consisted of 150 mM KCl, 6 mM $MgCl_2$, 5 mM *N*-[2-hydroxyethyl]piperazine-*N*′-[2-ethanesulfonic acid] (HEPES), and 4 mM ethylene glycol bis(2-aminoethyl ether)-*N*,*N*,*N*′,*N*′-tetraacetic acid (EGTA) at pH 7.4. Ice-cold lysis medium contained 10 mM tris-(hydroxymethyl)aminomethane hydrochloride (Tris-HCl) and 1 mM EGTA at pH 7.4. Stopper solution consisted of ice-cold kaline, 10 μM cytochalasin B (CCB), and 100 μM phloretin; RQF stopper solution contained ice-cold kaline, 20 μM CCB, and 200 μM phloretin. Phosphate-buffered saline consisted of 145 mM NaCl and 20 mM sodium phosphate. Sample buffer (2×) contained 125 mM Tris-HCl at pH 6.8, 4% sodium dodecyl sulfate (SDS), 20% glycerol, and 50 mM dithiothreitol.

RBC Preparation. Red cells were isolated from whole human blood by repeated wash/centrifugation cycles. A total of 1 volume of whole blood was mixed with 20 volumes of ice-cold kaline and centrifuged at 5443*g* for 10 min at 4 °C. The serum and white buffy coat were aspirated, and the cycle was repeated until the supernatant was clear and the buffy coat was no longer visible. When depletion of endogenous intracellular sugar was required, cells were resuspended in 20 volumes of kaline and incubated for 30 min at 37 °C.

Red Cell Ghost Preparation. Washed red cells were mixed with 50 volumes of ice-cold hypotonic lysis buffer, and the suspension was gently stirred for 10 min at 4 °C. Red cell membranes were harvested by centrifugation at 18566*g* for 15 min, followed by two additional washes in lysis buffer and centrifugation steps. Membranes were resealed in 20 volumes of kaline medium for 30 min at 37 °C, containing or lacking 4 mM ATP at pH 7.4. Resealed ghosts were harvested using the same centrifugation settings and stored on ice for no more than 24 h.

Red Cell Integral Membrane Proteins (IMPs). Peripheral proteins were displaced from red cell membranes by exposing unsealed erythrocyte ghosts to 2 mM ethylenediaminetetraacetic acid (EDTA) and 15.4 mM NaOH at pH 12 at a concentration of 0.8 mg of protein/mL for 10 min at 4 °C. Membranes were collected by centrifugation at 18566*g* for 20 min at 4 °C. The pH of the membrane suspension was restored by 3 wash/centrifugation cycles in 5 volumes of Tris-HCl medium. The final protein concentration of the membrane suspension was adjusted to 2 mg/mL in Tris-HCl, and membranes were stored at −20 °C (prior to use within 24 h) or at −80 °C (for longer storage intervals).

Benchtop Sugar-Transport Measurements. The time course of [^{3}H]-3MG uptake by red cells and red cell ghosts was measured at 4, 12, and 20 °C as described previously (*27*). Briefly, 50 or 100 μL of cells or ghosts were exposed to unlabeled sugar with trace amounts of [^{3}H]-labeled sugar. Uptake was allowed to proceed over intervals as short as 10 s to equilibrium intervals of up to 8 h (at 4 °C, with high

concentrations of cold sugar). The addition of 10 volumes of ice-cold stopper solution to the reaction suspension was used to quench the transport reaction. Cells were pelleted by centrifugation for 1 min (Fisher Scientific, Model 235C microcentrifuge; 14000*g*), washed for a second time in stopper solution, and pelleted again via a second spin for 1 min. The contents of the isolated cells were released upon addition of 1 mL of 3% perchloric acid (PCA), and clarified by centrifugation, and two 400-μL aliquots of supernatant were transferred to scintillation vials, mixed with scintillation fluid, and counted in a Beckman scintillation spectrophotometer (LS6500).

Rapid Quench-Flow Sugar-Transport Measurements The time course of [^{3}H]-3MG uptake by red cells and red cell ghosts was measured at 4 and 20 °C by the RQF-63 rapid quench-flow system (Hi-Tech Scientific), as described previously (*28*). Briefly, this instrument permits precise control of the processes of reagent *mixing* (radiolabeled sugar and cells), *delay* (reagents sit in a reaction loop, where the length of the loop and reactant flow rate determine the total reaction time), and *quenching* (addition of the stopper solution) to complete an uptake assay. Stopper solution was maintained at 4 °C for all uptake experiments at all temperatures. The reaction sample is collected manually in 1 mL of stopper solution and processed as in conventional transport assays. The RQF was calibrated for temporal accuracy by monitoring the alkaline hydrolysis of dinitrophenolacetate (DNPA), a reaction that forms dinitrophenol and acetate. Using HCl (1 M) as the stopper solution and DNPA (88 μM) and NaOH (0.5 M) as the reactants, half-lives of 38.5 ± 3.9 and 178 ± 9 ms were obtained for DNPA hydrolysis at 22 and 4 °C, respectively. These results are consistent with an E_a (activation energy) for DNPA hydrolysis of 14.7 kcal mol^{-1} K^{-1} and extrapolate to the expected $t_{1/2}$ for DNPA hydrolysis at 25 °C of 25 ms (*29*).

Equilibrium Sugar Spaces. Washed RBCs and resealed ghosts were incubated with 50 μM 3MG, with trace radiolabel for 2 h at 4 °C, at which point equilibrium 3MG distribution was reached. The incubation time was increased up to 8 h when 3MG stock concentrations exceeded 10 mM. The reaction was quenched, and the samples were processed as described for conventional transport assays.

Fractional equilibration at each time point (FE_t) was calculated using the following equation:

$$FE_t = \frac{dpm_t}{dpm_{equilibrium}}$$

where dpm_t represents disintegrations per minute (amount of [^{3}H]-3MG) at time t and $dpm_{equilibrium}$ describes disintegrations per minute (amount of [^{3}H]-3MG) when the reaction has attained equilibrium. This calculation normalizes results for variations in cell dilutions and radioisotope-specific activity across multiple experiments.

Sugar Occlusion. Washed RBCs were lysed in the presence or absence of 4 mM MgATP. Cells were then incubated at 4 °C in lysis medium with 50 μM 3MG plus trace radiolabel for sufficient time (>2 h) to ensure equilibrium 3MG binding with GluT1. Reactions were stopped by addition of 50 volumes of ice-cold stopper and processed as per usual methods. In lysed ghost experiments, the reaction was stopped with lysis buffer containing or lacking 10 μM CCB and 100 μM phloretin. In experiments using IMPs, kaline buffer replaced lysis buffer and contained no inhibitors, CCB (10 μM), phloretin (100 μM), or CCB and phloretin. IMPs were subject to trypsin digestion at a 1:30 trypsin/protein ratio for 15 min at 37 °C, as described previously (*30*). Proteolysis was stopped by addition of a complete EDTA-free protease inhibitor cocktail (Roche). Parallel null digestions received equivalent volumes of trypsin-free kaline and protease inhibitor.

Equilibrium CCB Binding. CCB binding to red cells and stripped ghosts was measured as described previously (*20*). Briefly, 50 μL of cells were mixed with 50 μL of radiolabeled CCB, in the presence of increasing concentrations of unlabeled CCB. Two 10-μL aliquots were removed for counting (totals). The suspension was incubated with rotation at 4 °C for 30 min by which time equilibrium binding was achieved. The suspension was centrifuged for 1 min, and two 10-μL aliquots of the supernatant were removed for counting (free) counts. Bound CCB is computed as the total counts minus the free counts. Cytochalasin D (CCD, 10 μM) was included in all solutions to inhibit CCB binding to non-GluT1 sites.

Analytical Procedures. Protein concentrations were determined by the Pierce BCA procedure. Enzyme-linked immunosorbent assays (ELISA) confirmed that membrane suspensions contained equivalent amounts of GluT1. C-Ab and goat anti-rabbit HRP conjugate antibodies served as the primary and secondary antibodies, respectively. ELISA reactions were developed with Pierce 1-step ATBS developing solution and analyzed by using a Bio-Rad Laboratories Benchmark Microplate Reader. SDS-slab (10%) polyacrylamide gel electrophoresis (PAGE) and Western blot analysis of proteins using C-Ab of membrane proteins were performed as described previously (*31*). Red cell counts were obtained by using a standard curve of cell suspension hemoglobin absorbance at 417 nm versus manual cell counts obtained using a hemocytometer. ATP was measured in neutralized PCA extracts of cells and red cell ghosts using a luciferin−luciferase assay kit purchased from Molecular Probes (Eugene, OR).

Calculation of Transport Constants. Radiolabeled sugar uptake by cells and ghosts (time-course data) were fitted to a three-compartment (phase) equation:

$$S_t = C_r(1 - e^{-k_r t}) + C_f(1 - e^{-k_f t}) + C_s(1 - e^{-k_s t})$$

where S_t is the sugar associated with the cells at time t, C_r, C_f, and C_s represent equilibrium sugar spaces associated with rapid, fast, and slow cell compartments or transport phases, respectively, and k_r, k_f, and k_s are first-order rate constants describing the rate of equilibration of rapid, fast, and slow compartments/phases, respectively. V_{max} and $K_{m(app)}$ for 3MG uptake were computed using direct, nonlinear regression analysis of the sugar concentration dependence of 3MG uptake assuming simple Michaelis−Menten kinetics. Arrhenius plots (ln k versus 1/T) were fitted by linear regression using the equation:

$$\ln k_n = \ln A + \frac{E_a}{RT}$$

where k_n is the rate constant for rapid, fast, or slow phases of uptake, A is the Arrhenius constant, R is the gas constant

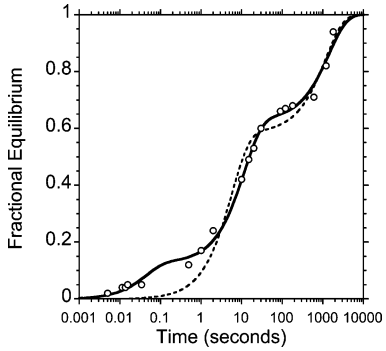

FIGURE 1: 3-*O*-Methylglucose uptake by human erythrocytes at 22 °C. Ordinate, 3MG uptake reported as fractional equilibration. Abscissa, time in seconds. The dashed and solid curves were computed by nonlinear regression and represent the time course of net 3MG uptake assuming that transport consists of a double or triple exponential process, respectively. The two exponent fit fails to account for the rapid phase. The following constants were obtained for the double exponential: $C_r = 0.58$, $k_r = 0.17$ s^{-1}, $C_f = 0.42$, and $k_f = 0.0008$ s^{-1}. Constants describing the triple exponential are $C_r = 0.13$, $k_r = 22.6$ s^{-1}, $C_f = 0.50$, $k_f = 0.086$ s^{-1}, $C_s = 0.37$, and $k_s = 0.0007$ s^{-1}. Each data point represents the mean of three measurements made in three separate experiments.

(1.987 cal K^{-1} mol^{-1}), and E_a is the activation energy (kcal mol^{-1}). The slope (E_a/R) is obtained by linear regression analysis. The software program KaleidaGraph (version 3.6, Synergy Software) was used to plot all data and compute best fit parameters for each curve fit.

RESULTS

Time Course of 3MG Uptake. 3MG uptake by RBCs has been reported to be a biphasic process (*11*). With the extended temporal resolution provided by the RQF, it is now evident that curve fitting with a two-exponent rate equation does not adequately describe the most rapid transport process. The time course of 3MG uptake by erythrocytes at 22 °C (0.01−3600 s) is best described by a three-exponent fit (Figure 1). This analysis describes net transport as the sum of either three parallel or three sequential processes. These processes are the rapid filling of a small compartment, fast filling of a large compartment, and slow filling of a large compartment.

The temperature dependence of 3MG net import by erythrocytes is summarized in Figure 2. The size of each compartment and the corresponding rates of compartment filling are significantly affected by reduced temperature. The rapid process is inhibited by 50-fold upon lowering the temperature from 22 to 4 °C, whereas the relative size of the slow process is increased with decreasing temperature. Only conventional assays could be performed at 12 °C because the RQF was not easily adjusted to this temperature. Arrhenius analysis of the temperature dependence of the rate of each process is presented in Figure 3. Rapid, fast, and slow phases are characterized by activation energies of 44.6 (two temperature points only), 20.9 ± 5.9, and 20.8 ± 6.7 kcal mol^{-1}, respectively. In comparison, E_a for the simple self-diffusion of glucose in aqueous solution is 5.1 kcal mol^{-1} (*16*). This suggests that neither the rapid, fast, nor slow processes are diffusion-limited reactions.

Time Course of 3MG Uptake in the Presence of Inhibitors. CCB interacts with the sugar exit site of GluT1, serving as a competitive inhibitor of sugar exit and as a noncompetitive

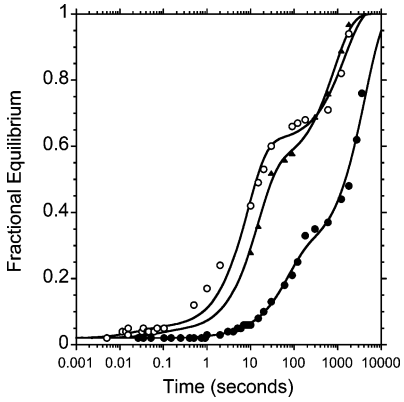

FIGURE 2: Temperature dependence of 3-*O*-methylglucose uptake by human erythrocytes at 4 (●), 12 (▲), and 22 °C (○), respectively. Ordinate, 3MG uptake reported as fractional equilibrium. Abscissa, time in seconds. Uptakes at 4 and 22 °C are fit with a three-exponent curve, and the 12 °C data do not include the rapid (earliest) phase of 3MG uptake data. All data are superimposed on a background of 0.02. Each point represents the mean of three independent experiments. The following rate constants were obtained: at 4 °C, $C_r = 0.01$, $k_r = 0.277$ s^{-1}, $C_f = 0.248$, $k_f = 0.0147$ s^{-1}, $C_s = 0.742$, and $k_s = 0.000\,236$ s^{-1}; at 12 °C, $C_r = 0.03$ and $k_r = 6.8$ s^{-1} (represent values estimated from Arrhenius plot, not obtained directly), $C_f = 0.502$, $k_f = 0.0675$ s^{-1}, $C_s = 0.468$, and $k_s = 0.001\,21$ s^{-1}; and at 22 °C, $C_r = 0.03$, $k_r = 38.76$ s^{-1}, $C_f = 0.562$, $k_f = 0.115$ s^{-1}, $C_s = 0.408$, and $k_s = 0.000\,687$ s^{-1}.

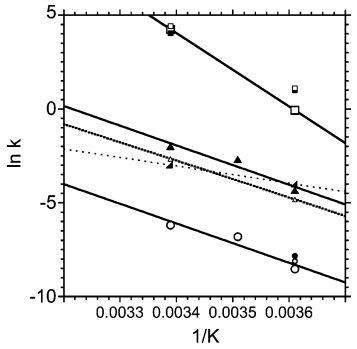

FIGURE 3: Arrhenius plot examining temperature dependence of 3-*O*-methylglucose uptake rates. Ordinate, natural log of rate constants from Figure 2. Abscissa, 1/temperature in per kelvin. The straight lines drawn through the points were computed by linear regression. The activation energies of each of the three phases are obtained from the slope of each plot as described in the Materials and Methods: rapid (□), 44.6 kcal mol^{-1}; fast (▲), 20.9 ± 5.9 kcal mol^{-1}; and slow (○), 20.8 ± 6.7 kcal mol^{-1}, respectively. Data are also shown for RBC ghosts lacking (small □, small △, and small ○) or containing 4 mM ATP during resealing (small ■, small ▼, and ●). Ghost data summarize rate constants for rapid (□), fast (▲), and slow (○) phases of uptake.

inhibitor of sugar uptake (*32*, *33*). Extracellular maltose is not transported by GluT1 but interacts with the glucose import site to competitively inhibit sugar uptake (*32*). The time course of 3MG uptake by RBCs at 4 °C is severely inhibited in the presence of 50 μM CCB (Figure 4A) and 50 mM maltose (Figure 4B). These results indicate that all three transport phases are subject to inhibition by specific inhibitors of carrier (protein)-mediated sugar transport. This result is expected if uptake were described by three, independent (parallel), carrier-mediated processes. This result would also be produced if net transport were described by three sequential (dependent) processes in which all three processes are carrier-mediated and inhibited by CCB. This result is not expected if only the first or second phases of

Table 1: 3MG Uptake Kinetics in Red Cells and Ghosts

		compartment[a]					
		rapid		fast		slow	
cells	temperature (°C)	k_{rapid}[b] (s^{-1})	C_{rapid}[c] (fraction)	k_{fast}[b] (s^{-1})	C_{fast}[c] (fraction)	k_{slow}[b] (s^{-1})	C_{slow}[c] (fraction)
intact cells	4	0.94 ± 0.26	0.036 ± 0.006	0.013 ± 0.001	0.27 ± 0.03	0.000 20 ± 0.000 03	0.71 ± 0.02
	12	6.76[d]	0.03	0.067 ± 0.001	0.502 ± 0.016	0.0011 ± 0.0001	0.468 ± 0.016
	22	69.7 ± 17.5	0.037 ± 0.004	0.13 ± 0.01	0.51 ± 0.08	0.0021 ± 0.0015	0.45 ± 0.09
ghosts and ATP	4	2.73 ± 0.77	0.071 ± 0.016	0.0183 ± 0.009	0.594 ± 0.030	0.0004 ± 0.0001	0.335 ± 0.046
	22	56.83 ± 26.16[e]	0.058 ± 0.026[e]	0.050 ± 0.012[e]	0.942[e]		
ghosts and 0 ATP	4	3.02 ± 1.47	0.122 ± 0.013	0.008 ± 0.0023	0.3913 ± 0.022	0.0003 ± 0.000 04	0.4867 ± 0.035
	22	82.80 ± 25.96[e]	0.043 ± 0.017[e]	0.069 ± 0.017[e]	0.958[e]		

[a] The time course of 50 μM 3MG uptake was measured in red cells and red cell ghosts containing or lacking 4 mM exogenous MgATP. Uptake data were analyzed assuming three phases of uptake, rapid, fast, and slow (see Figures 1, 2, and 5). [b] k is the first-order rate constant describing the rate of compartment filling (per second). [c] C is the compartment size as a fraction of the total cellular 3MG space. [d] Experiments made at 12 °C did not permit determination of the kinetics of filling of the rapid compartment. These numbers were obtained by extrapolation from Arrhenius analysis of the temperature dependence of transport (see Figure 3). [e] These analyses were made before we recognized that uptake was consistent with a three-compartment model. Time points were not obtained over a sufficiently broad time range to accurately determine k_s and C_s. The data are therefore analyzed assuming only two components of uptake, rapid and fast. These data represent the mean ± SEM of at least three separate determinations made 3 times.

three sequential processes are inhibited. Here, only the inhibited phases should show reduced rates of progression.

Monophasic 3MG uptake by red cells in the presence of CCB also suggest that the population of cells employed in these studies is uniform with respect to the surface area/volume ratio. The rate constant, k, for trans-bilayer diffusion of a molecule into a cell of radius r is directly proportional to the product PA, where P is the permeability coefficient (cm s^{-1}) for trans-bilayer diffusion of the molecule and A is the surface area/volume ratio (cm^{-1}) of the cell (*34*). Assuming that P is constant for all red-cell-derived, membrane-bound vesicles, k is directly proportional to A. For a spherical body, the surface area/volume ratio is $A = 3/r$ [red cells are biconcave disks, but membrane vesicles formed from red cells are predominantly spherical (*35*, *36*)]. Thus, for rapid, fast, and slow rate constants of 69.7, 0.13, and 0.0021 s^{-1} (22 °C, Table 1), the relative A values are 3.4×10^3, 66, and 1, respectively. If the slowest phase corresponds to the radius of an erythrocyte (3.5 μm), the rapid and fast phases would correspond to uptake by cells with radii of 0.1 and 45.7 nm, respectively. Thus, a mixture of three cell populations of these sizes is also expected to display rapid, fast, and slow phases of transmembrane sugar diffusion.

Time Course of 3MG Uptake in Resealed, Hypotonically Lysed Cells. At 22 °C, the slowest phase of net sugar uptake is 32 000-fold slower than the most rapid phase of uptake. This raises the interesting possibility that the slow phase of sugar import may reflect some process other than sugar release into cytosolic water. 3MG, like D-glucose, can nonenzymatically glycate cellular proteins (*37*). The slow phase may therefore represent 3MG interaction with cellular proteins to form glycated proteins or noncovalent precursors to glycated proteins (*37*). If 3MG interaction with cytosolic proteins accounts for the slow phase of net uptake, the use of resealed erythrocyte ghosts, which lack more than 90% of cytosolic proteins, should diminish this phase of transport.

The kinetics of 3MG net uptake by resealed red blood ghosts at 4 °C are not significantly different from those observed in intact cells (Table 1 and Figure 5). This observation refutes the hypothesis that the slow phase of uptake results from 3MG interaction with cytosolic proteins. Sugar that is transported into the cell is also fully recoverable

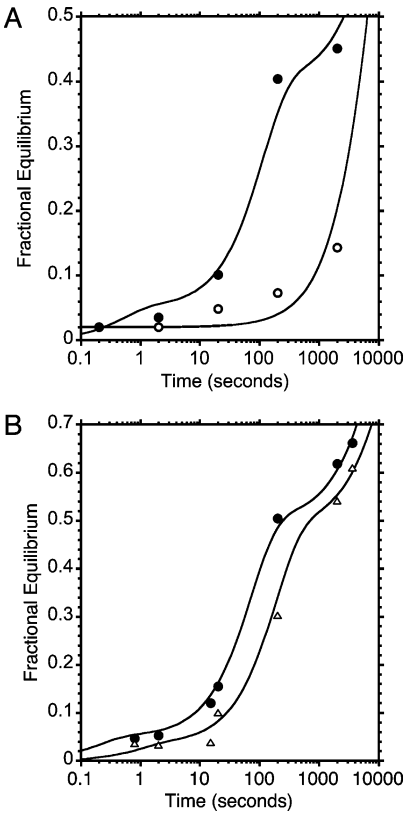

FIGURE 4: (A) 3-*O*-Methylglucose uptake by human erythrocytes in the presence of transport inhibitor CCB at 4 °C. Ordinate, 3MG uptake reported as fractional equilibrium. Abscissa, time in seconds. Control uptake (●) in the absence of CCB differs greatly from uptake where the red cells and 3MG were previously exposed to 50 μM CCB (○). At all measured time points, a substantially higher fractional equilibrium is reached when uptake is uninhibited. The curves drawn though the points have the following constants: control, $C_r = 0.05$, $k_r = 5\ s^{-1}$, $C_f = 0.45$, $k_f = 0.014\ s^{-1}$, $C_s = 0.5$, $k_s = 11.8 \times 10^{-5}\ s^{-1}$, $R^2 = 0.997$; and CCB, $C_s = 1$, $k_s = 0.0002\ s^{-1}$, background = 0.02, $R^2 = 0.567$. (B) 3-*O*-Methylglucose uptake by human erythrocytes in the presence of competing sugar maltose at 4 °C. Control uptake (●) proceeds more rapidly than uptake in the presence of 50 mM (△) maltose. The curves drawn though the points have the following constants: control, $C_r = 0.05$, $k_r = 2\ s^{-1}$; $C_f = 0.35$, $k_f = 0.009\ s^{-1}$, $C_s = 0.6$, $k_s = 7.3 \times 10^{-5}\ s^{-1}$, $R^2 = 0.989$; and 50 mM maltose, $C_r = 0.035$, $k_r = 1\ s^{-1}$, $C_f = 0.45$, $k_f = 0.0054\ s^{-1}$, $C_s = 0.515$, $k_s = 7.0 \times 10^{-5}\ s^{-1}$, $R^2 = 0.991$.

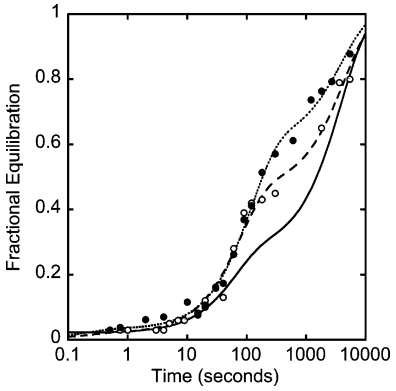

FIGURE 5: 3-*O*-Methylglucose uptake at 4 °C by human erythrocyte ghosts containing (●) or lacking (○) 4 mM ATP, respectively. Ordinate, 3MG uptake reported as fractional equilibrium. Abscissa, time in seconds. Uptake is fitted with a three-exponent curve. The following rate constants were obtained from averages of three independent experiments: 4 mM ATP (•••), $C_r = 0.01$, $k_r = 0.277$ s^{-1}, $C_f = 0.248$, $k_f = 0.0147$ s^{-1}, $C_s = 0.742$, $k_s = 0.000\,236$ s^{-1}; and 0 ATP (- - -), $C_r = 0.03$ and $k_r = 13.1$ s^{-1} (represent values estimated from Arrhenius plot, not obtained directly), $C_f = 0.502$, $k_f = 0.0675$ s^{-1}, $C_s = 0.468$, $k_s = 0.001\,21$ s^{-1}. The time course of 3MG uptake in red cells at 4 °C (Figure 2) is also shown for comparison (—).

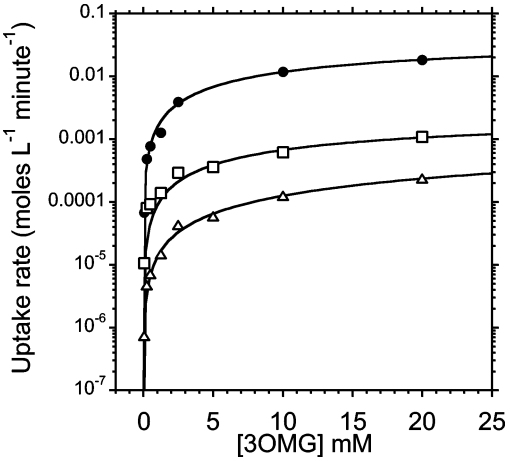

FIGURE 6: 3-*O*-Methylglucose concentration dependence of sugar uptake in human erythrocytes as measured at 4 °C. Ordinate, uptake rate of 3MG (mol L^{-1} min^{-1}). Abscissa, 3MG concentration in uptake solution, mM. 3MG uptake rates were measured at three time points corresponding to rapid (0.125 min), fast (0.5 min), and slow (30 min) phases of sugar transport. The transport parameters at each time point are reported as follows: rapid phase (●), $V_{max} = 40.3 \pm 16.0$ mmol (L of cell water)$^{-1}$ min^{-1}, $K_m = 22.6 \pm 10$ mM, $R^2 = 0.998$; fast phase (□), $V_{max} = 2.4 \pm 0.5$ mmol (L of cell water)$^{-1}$ min^{-1}, $K_m = 22.7 \pm 6.2$ mM, $R^2 = 0.982$; and slow phase (△), $V_{max} = 1.33 \pm 0.02$ mmol (L of cell water)$^{-1}$ min^{-1}, $K_m = 94.2 \pm 4.5$ mM, $R^2 = 0.997$.

during sugar export (*11*, *38*), indicating that 3MG does not form a covalent complex with cellular molecules.

Experiments at 22 °C were performed before it was recognized that three phases of uptake exist. These data were analyzed assuming two phases of uptake, and because insufficient time points were collected at longer times (200−10 000 s), the data do not permit accurate determination of constants for filling of the slow compartment. Compartment size and rates of compartment filling in red cell ghosts lacking exogenous ATP at 4 °C are not significantly different from those measured in intact red cells. The intact cells used in these specific measurements had been stored at 4 °C for a prolonged period (>14 days), suggesting that they may have become metabolically depleted. Exogenous, intracellular ATP (4 mM) increases the size of the fast compartment at the expense of the slow compartment in resealed cells (Figure 5). Analysis of cellular ATP content indicates that ATP-free ghosts are nominally ATP-free, while intact cells contain significantly lower ATP levels (0.7 mM) than ghosts containing exogenous ATP (3.8 mM). These data strongly suggest that prolonged cold storage of human blood results in significant depletion of intracellular ATP levels.

The temperature dependence (4 and 22 °C) of 3MG net import by resealed erythrocyte ghosts is summarized in Figure 3 and Table 1. The rapid process (k_r) is indistinguishable from that of intact red cells. The fast process in ghosts appears to have somewhat reduced (2-fold) temperature sensitivity relative to the fast process in intact cells. This is manifest as indistinguishable k_f in cells and ghosts at 4 °C but slightly lower k_f in ghosts at 22 °C. At 4 °C, the slow processes (k_s) in intact cells and red cell ghosts are indistinguishable.

Concentration Dependence of Sugar Uptake. V_{max} and $K_{m(app)}$ parameters for sugar uptake are, in principle, computed by using initial rates of net sugar transport. RBC 3MG uptake at 4 °C was measured during rapid (0.125 min), fast (0.5 min), and slow (30 min) phases of uptake (Figure 6). V_{max} and $K_{m(app)}$ values computed for uptake during the rapid transport phase are 42.6 ± 4.2 mmol (L of cell water)$^{-1}$ min^{-1} and 26.5 ± 4.1 mM, respectively. V_{max} and $K_{m(app)}$ for uptake during the fast phase are 2.5 ± 0.6 mmol (L of cell water)$^{-1}$ min^{-1} and 27.5 ± 10.7 mM, respectively. V_{max} and $K_{m(app)}$ for uptake during the slow transport phase are 1.97 ± 1.01 mmol (L of cell water)$^{-1}$ min^{-1} and 148.2 ± 84.5 mM, respectively. V_{max} for sugar uptake is approximately 15-fold greater when computed using rapid time points rather than fast incubation intervals. $K_{m(app)}$ values are similar when measured during rapid and fast phases and 6-fold higher when measured during the slow phase.

3MG Concentration Dependence of k_r. Figure 7 summarizes the [3MG] dependence of k_r and C_r. k_r is independent of [3MG], but the size of the rapid compartment (C_r) increases in a saturable manner with [3MG]. The maximal size of C_r is 1.94 nmol/mg of membrane protein, and the compartment is 50% filled at 340 μM 3MG.

Is Sugar Occluded by GluT1? Previous equilibrium sugar-binding experiments have demonstrated that 2 mol of 3MG are bound per mol of GluT1 (*27*). Only one of these sites is inhibited by CCB. In the present study, we considered the possibility that the rapid phase of net sugar uptake corresponds to CCB and phloretin-dependent sugar occlusion within the translocation pathway. If correct, occlusion may be measurable in lysed (unsealed) ghosts and in IMPs as the ability of membranes to retain sugar following removal of unbound sugar by multiple ice-cold washes in the presence of the transport inhibitors, CCB and phloretin.

Ghosts lysed in the presence of Mg or MgATP and incubated in lysis medium containing 3MG retain more sugar upon washing in sugar-free stopper solution than do ghosts lysed in the absence of MgATP. MgATP-containing ghosts, however, characteristically display higher absorbance at 417 nm and higher total protein amounts, despite ELISA analysis confirmation that all cells contain the same amount of GluT1.

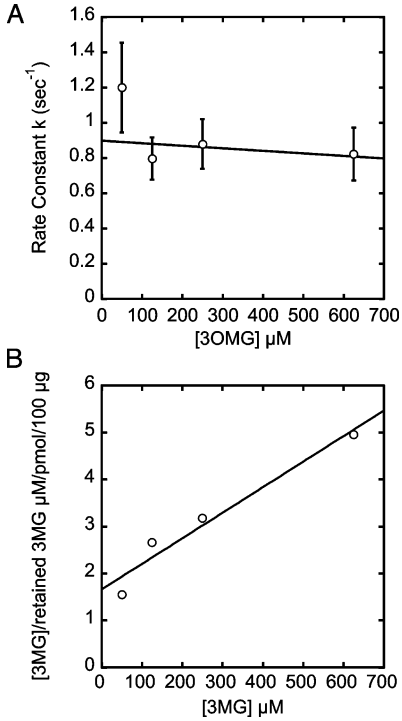

FIGURE 7: 3-*O*-Methylglucose concentration dependence of k_r and C_r at 4 °C. 3MG (50, 125, 250, and 625 μM) uptake was measured during the first 2 s following mixing. k_r and C_r were computed by nonlinear regression and are plotted as a function of [3MG]. (A) Dependence of k_r on 3MG. Ordinate, k_r, in s^{-1}. Abscissa, [3MG] in micromolar. The results of two or more separate experiments made 3 times are shown as the mean ± standard error of the mean (SEM). The straight line drawn through the points was computed by nonlinear regression (assuming k_r = intercept + constant[3MG]) and was weighted by the SEM of each data point. The results were intercept = (0.90 ± 0.12) s^{-1}, constant = (0.000 14 ± 0.000 36) μM^{-1} s^{-1}, and R^2 = 0.074. (B) Dependence of C_r on 3MG. Ordinate, [3MG] per pmol of 3MG retained per 100 μg of membrane protein (μM 3MG (pmol of 3MG retained)$^{-1}$ (100 μg of membrane protein)$^{-1}$); Abscissa, [3MG] in micromolar. This is a Hanes−Woolfe analysis of 3MG retention by red cell IMPs. The results of two or more separate experiments made 3 times are shown as the mean. The straight line drawn through the points was computed by nonlinear regression (assuming C_r = intercept + constant[3MG]). The results are intercept = (1.74 ± 0.34) μM 3MG (pmol of 3MG retained)$^{-1}$ (100 μg of membrane protein)$^{-1}$, constant = (0.0051 ± 0.0009) μM 3MG (pmol of 3MG retained)$^{-1}$ (100 μg of membrane protein)$^{-1}$, and R^2 = 0.953.

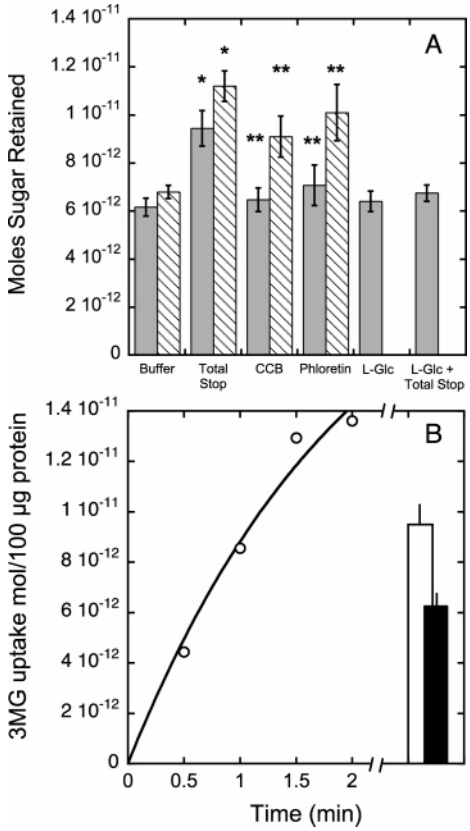

FIGURE 8: (A) 3-*O*-Methylglucose retention by red cell IMPs at 4 °C after arresting equilibrium reactions (50 μM 3MG or 50 μM L-glucose plus 100 μg of IMPs) with buffer or buffer plus transport inhibitors. Ordinate, sugar retention measured in moles of sugar per 100 μg of membrane protein. Abscissa, equilibrium transport reaction stop conditions. In control nontrypsin-treated cells (solid bar), stopping the reaction with complete CCB/phloretin-quench solution results in the statistically significant increase of 3.3 pmol of 3MG retained versus stopping the reaction with kaline buffer. In trypsin-treated IMPs (dashed bar), stopping the reaction with complete quench, CCB, and phloretin results in the statistically significant increase of 4.4, 2.3, and 3.3 pmol of 3MG retained versus stopping the reaction with kaline buffer. Trypsinized membranes retain 3MG more effectively than do control membranes. L-Glucose retention ± quench (CCB and phloretin) were not significantly different from 3MG in the absence of quench. (B) Quantitative comparison of 50 μM 3-*O*-methylglucose uptake by red cells and retention by red cell IMPs at 4 °C. Ordinate, sugar uptake by red cells or retention measured in moles of sugar per 100 μg of membrane protein. Abscissa, time in minutes. The open circles show the time course of 3MG uptake by cells. The curve drawn through the points is a single exponential with the following constants: C_r = (22.6 ± 8) pmol/100 μg of protein; k_r = 0.5 ± 0.2 s^{-1}. The open bar represents the equilibrium (±SEM) 3MG retention space of IMPs when quenched with CCB and phloretin. The filled bar represents the equilibrium (±SEM) 3MG retention space of IMPs when quenched with inhibitor-free buffer.

It is possible, therefore, that this effect is due to decreased lysis efficiency in the presence of MgATP. To avoid this pitfall, sugar occlusion experiments were repeated using IMPs. These membranes are enriched in GluT1 content and are osmotically inactive, and both cytosolic and extracellular GluT1 domains are quantitatively accessible to peptide-directed IgGs (*9*, *39*). This confirms that IMPs do not form sealed proteoliposomes under these conditions. As with ghost membranes, the presence of transport inhibitors in the wash solution promotes sugar retention by IMPs (Figure 8).

GluT1 digestion by intracellular trypsin is known to inhibit red cell sugar transport (*40*). We hypothesized that trypsin would also inhibit 3MG occlusion by RBC IMPs because of proteolytic modification of sugar- and inhibitor-binding sites. 3MG retention at 4 °C by native and trypsinized IMPs are not significantly different (Figure 8A). CCB binding by IMPs is not significantly altered by trypsinization (control, B_{max} = 0.72 ± 0.19 nmol/mg of membrane protein, $K_{d(app)}$ = 72 ± 30 nM; trypsin, B_{max} = 1.01 ± 0.25 nmol/mg of membrane protein, $K_{d(app)}$ = 177 ± 55 nM). A second round of exposure of control and trypsin-treated IMPs to conditions that disrupt salt bridges (alkaline wash medium) does not significantly diminish CCB binding to IMPs. Immunoblot analysis of IMPs using GluT1 carboxy-terminal peptide-directed Abs (C-Abs) confirms that trypsin quantitatively cleaves GluT1 carboxy-terminal domains (not shown).

Sugar retention appears to be enhanced by stopper solutions in trypsinzed versus control cells. Retention measurements made using radiolabeled L-glucose (a nonreactive

substrate) indicate no enhancement of sugar retention in the presence of CCB and phloretin. L-Glucose retention by IMPs is quantitatively indistinguishable from 3MG retention in the absence of CCB and phloretin (Figure 8A). These observations suggest that CCB- and phloretin-dependent 3MG retention is a GluT1-mediated event. Figure 8B compares the amount of 3MG retained by IMPs (±quench) to the rapid time course of 50 μM 3MG uptake by red cells at 4 °C.

DISCUSSION

Three Sequential Phases of Glucose Transport. The experiments presented in this study indicate that monosaccharide import by erythrocytes is comprised of at least three phases. Multiphasic uptake is consistent with two possibilities. (1) There are three distinct populations of red cells characterized by different sizes or different GluT1 content. (2) There is a single cell population containing three serial compartments through which a sugar molecule must pass to equilibrate with the total cellular space.

Several observations argue against the first hypothesis. These include (1) rejection of multiple cell sizes by the observation of monophasic 3MG uptake in cells when transport is inhibited by CCB (Figure 4A and ref *11*); (2) the extreme range of cell sizes (0.1 nm−3.5 μm radii, see the Results) that would be necessary to explain the findings; and (3) monophasic sugar exit from red cells over time courses corresponding to the fast and slow phases of uptake [(*11*, *41*, *42*) Leitch and Carruthers, unpublished]. The latter observation excludes the possibility that some red cells possess greater sugar-transport capacity than other cells in the same population. We therefore conclude that the three phases of protein-mediated sugar import correspond to three processes that occur sequentially.

What Are the Three Measurable Glucose Transport Phases? Rapid, fast, and slow phases of 3MG uptake by red cells are retained in red cell ghosts. This indicates that all three phases are associated with the red cell membrane and are independent of sugar interaction with cytoplasmic proteins. This does not exclude the possibility that 3MG interacts with other membrane-associated proteins following release from the glucose transporter.

Rapid Phase. The 3MG uptake experiments presented in Figures 2 and 3 show that all phases of sugar translocation are temperature-sensitive. The high activation energy of the rapid phase indicates that this phase presents the greatest energy barrier to sugar import. Each transport phase is inhibited by specific inhibitors of GluT1-mediated sugar transport. This result is expected if transport proceeds through serial steps and all three steps are sensitive to the inhibitor. The CCB and phloretin-dependent 3MG space "occluded" in or retained by unsealed red cell ghosts and by IMP suspensions is quantitatively most similar to the smallest and most rapid phase of sugar uptake by cells. The sugar concentration dependence of the size of this phase indicates simple, saturable kinetics with a 3MG capacity of 1.94 nmol/mg of membrane protein and $K_{d(app)} = 340$ μM. This sugar-binding capacity is indistinguishable from the sugar-inhibitable CCB-binding capacity of human red cells [0.9−1.5 nmol/mg of membrane protein (*27*, *43*)] but is somewhat greater than the measured 3MG retention of red cell membrane IMPs at 50 μM 3MG (see Figure 8B).

The time course of the rapid phase of 50 μM 3MG uptake at 4 °C extrapolates to an equilibrium 3MG space of 22.6 ± 8.1 pmol of 3MG per 100 μg of membrane protein. The quench-dependent 3MG retention space of IMPs at 50 μM 3MG is 3.2 ± 1.3 pmol/100 μg of protein. Assuming that the relative GluT1 content of IMPs is 1.67-fold greater than that of intact red cell membranes and that the rapid phase of uptake and 3MG retention by membranes represents the same process, this represents a retention efficiency of 10%. Low efficiency sugar retention could result from two factors: (1) in red cell experiments, sugar associated with the rapid phase of uptake is released into the wash-inaccessible, intracellular water, whereas in experiments with IMPs, the water content of the entire suspension is exchanged during washes; and (2) the transient nature of carrier interaction with the quenching agents (CCB and phloretin) may lead to a loss of carrier-sequestered sugars. CCB has an average dwell time on the e1 site of approximately 1 s at 4−10 °C [$1/k_{off}$ (*44*, *45*)]. While equivalent data do not exist for phloretin interaction with the e2 site, $K_{i(app)}$ for phloretin inhibition of GluT1 is approximately 10-fold greater than $K_{i(app)}$ for CCB inhibition of transport (*32*), suggesting that k_{off} for phloretin dissociation from the e2−phloretin complex may be even greater than k_{off} for CCB dissociation from e1−CCB. The lifetime of the rapid phase of 3MG import (0.3−1 s at 4 °C) is similar to the CCB dwell time on the carrier. It is probable, therefore, that a significant fraction of the sequestered 3MG is lost during multiple washes in the presence of CCB and phloretin.

k_r is independent of [3MG] (Figure 7A), suggesting that this step does not represent the second-order process of sugar binding to GluT1 in which k_r would be expected to increase linearly with [3MG] (*44*). We therefore propose that the rapid phase represents a conformational change following and promoted by 3MG binding to e2. This conclusion is also supported by estimates of the second-order encounter rate constant for 3MG interaction with GluT1 if the rapid phase of import was represented by the second-order reaction between 3MG and GluT1. If this were true, the pseudo-first-order rate constant (k_r) for this interaction at fixed [GluT1] is given (*44*) by

$$k_r = k_{off} + k_e[3MG]$$

where the rate constants k_{off} and k_e describe the reaction

$$\text{GluT1} + 3\text{MG} \underset{k_{off}}{\overset{k_e}{\rightleftharpoons}} \text{GluT1}-3\text{MG}$$

k_e is therefore obtained as

$$k_e = \frac{k_r - k_{off}}{[3MG]}$$

k_{off} for simple carrier-mediated transport is estimated (*3*) as

$$k_{off} = \frac{V_{max}^{exchange}}{[GluT1]}$$

where $V_{max}^{exchange}$ is the V_{max} for unidirectional sugar fluxes when $[3MG]_i = [3MG]_0$. Previous measurements of $V_{max}^{exchange}$ permit calculation of k_{off} as 40 s^{-1} at 4 °C and as 275 s^{-1} at 22 °C (*20*). Measurements of k_r reported here are 1 s^{-1} at 4

°C and 70 s^{-1} at 22 °C (Table 1). According to this analysis, k_e would have a negative value if k_r represents the second-order interaction between 3MG and GluT1. This is a physical impossibility. The pseudo-first-order rate constant describing 3MG interaction with GluT1 must be at least 4−40-fold greater than the first-order rate constants measured for the rapid phase of transport.

We suggest that the occluded 3MG space and the rapid phase of 3MG uptake by cells represent sugar occlusion within the sugar translocation pathway. The occluded 3MG space cannot be the previously reported ATP-dependent 3MG binding to GluT1 (*27*) because that reaction is inhibited by CCB and phloretin and is rapidly reversible. Bound 3MG would therefore be lost during multiple washes to remove unbound sugars.

Fast and Slow Phases. The fast and slow phases have lower temperature sensitivities than the rapid phase of net import. The activation energy for GluT1-mediated glucose transport in reconstituted proteoliposomes ranges between 5.1 and 23.7 kcal mol^{-1} [specific values are lipid composition-dependent (*46*)]. In human red cells, the activation energy for glucose transport is 18.4 kcal mol^{-1} (*47*, *48*). This latter value was obtained by measuring transport over intervals that correspond to the fast phase reported in the present study, where E_a is 20.9 ± 5.9 kcal mol^{-1}.

Previous studies from this laboratory have demonstrated the existence of a cytosolic 3MG occlusion mechanism in which an additional sugar-binding site within the glucose transporter is exposed upon GluT1 interaction with ATP (*27*). We propose that this binding phenomenon is associated with the fast phase of transport reported in the present study because 3MG equilibrium binding to the cytosolic site and the fractional size of the fast phase of 3MG uptake by red cells and red cell ghosts are both increased by cytoplasmic ATP [see Figure 5 and Table 1 and (*27*)]. We propose that the slow phase of net sugar import corresponds to the release of bound sugar from the GluT1 cytoplasmic sugar-binding site into bulk cytosol. It is also possible that the slow phase represents noncovalent 3MG interactions with RBC membrane proteins. Interactions with bulk cytosolic proteins are ruled out because the kinetics of slow compartment filling and the relative sizes of fast and slow compartments are retained in red cell ghosts.

Model for Glucose Transport. Resolution of the crystal structures of *Escherichia coli* LacY and GlpT transport proteins in the e1 (inward-facing) conformation has prompted the development of a model for lactose−proton symport (*12*, *18*). The model is a physical reinterpretation of the theoretical simple carrier, as proposed by Stein (*3*). The monomeric transporter first presents an import (e2) site. Upon lactose and proton binding, LacY undergoes a conformational change to the export (e1) configuration where sugar and proton are subsequently released. This mechanism presumes an intermediate conformation between e2 and e1 isomers in which the bound substrates are transiently sequestered within the closed translocation pathway and are neither accessible to interstitium nor cytosol. This translocation intermediate may resemble the occluded K and Na states of the NaKATPase (an e1e2ATPase) in which Na-dependent, ATP hydrolysis and K-binding-induced dephosphorylation promote conformational changes that temporarily occlude bound substrate from the aqueous milieu (*49*, *50*).

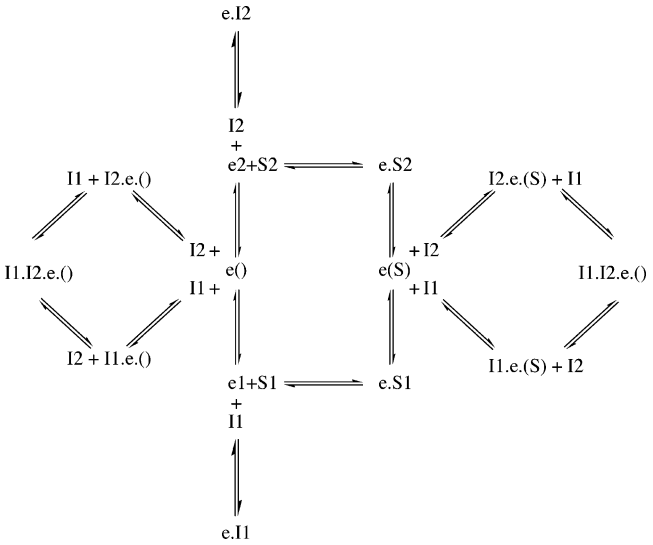

FIGURE 9: King−Altman scheme for sugar transport. The transporter, e, can exist in only one of three states in the absence of substrate (S) and ligands (I). e1 is the inward configuration of the carrier that presents a sugar-binding site to cytosol. e2 is the outward configuration of the carrier that presents a sugar-binding site to interstitium. The carrier isomerizes between the e1 and e2 states via the e() confomer. The e() confomer can bind extracellular (I2) and intracellular (I1) inhibitors simultaneously. e2 can interact only with extracellular inhibitor I2 or extracellular sugar S2. e1 can interact only with intracellular inhibitor I1 or intracellular sugar S1. eS1 isomerizes to eS2 via the occluded e(S) complex in which the sugar is trapped within the translocation pathway. As with e(), e(S) can interact with I1 and I2 simultaneously.

As with these preceding transport systems, the glucose transporter undergoes an analogous e2 ↔ e1 conformational change. This change, however, does not require ATP hydrolysis and can occur (although more slowly) in the absence of bound substrate. Sugar transport through a GluT1 subunit may proceed as follows (see Figure 9): (1) sugar binds to the e2 or external configuration to form eS2; (2) this event promotes a conformational change forming the translocation intermediate e(S); (3) when the transporter proceeds through e(S) to the eS1 state, the sugar dissociates into an internal cavity formed by GluT1 cytosolic domains, where it may bind to an ATP-dependent, noncatalytic sugar-binding site and thus remain within the confines of the protein; and (4) the sugar is released from the noncatalytic binding site back into the internal cavity or is released directly from eS1 into the cavity from which it diffuses (slowly in the presence of ATP) into bulk cytosol. We propose that the present study has examined phases two, three, and four, while phase one, the initial binding step, is refractory to the specific techniques of measurement used. It should be noted that this hypothesis predicts that ATP removal (e.g., formation of ghosts ± ATP_i) should reduce the size of the fast compartment (C_f) and increase the rate of release of sugar from the fast to slow compartments (reduce k_s). The former prediction is observed (Figure 5 and Table 1), but the latter is not, in part, perhaps because of the lack of precision in data. Future studies must address this prediction more closely.

If the rapid phase does indeed represent the formation of an e(S) state in which the sugar is occluded within the sugar-

transport pathway, this would mean that e(S) is capable of binding CCB and/or phloretin/extracellular maltose simultaneously. Indeed, it is possible to measure e(S) only in the presence of these inhibitors. A fundamental tenet of the simple carrier hypothesis is that CCB and maltose cannot bind to a carrier that contains a complexed transport substrate (*7*). However, we do know that GluT1 reacts simultaneously with CCB and phloretin (*7*). If the simple carrier hypothesis is correct, the ability of e(S) to bind phloretin and CCB would explain the experimental observations. A recent theoretical model of the GluT1 structure (*51*) suggests that intracellular CCB and extracellular phloretin docking sites may be simultaneously presented by each GluT1 subunit. A second possibility is that, in multimeric GluT1, 3MG can be occluded within one subunit, while the second subunit is locked into a dead-end conformation with CCB or phloretin. This hypothesis suggests a molar stoichiometry of 1 mol of CCB bound/mol of e(S), an assertion consistent with the results of this study.

It would be interesting to determine the effects of intracellular sugar on all three phases of unidirectional sugar uptake. Under infinite-trans uptake conditions (intracellular unlabeled [sugar] is high, and extracellular radiolabeled sugar levels are varied), the simple carrier hypothesis predicts that more e2 sites are available for interaction with extracellular sugar (S1 drives the carrier back to e2 via the eS1 → e(S) → eS2 export translocation pathway, which is faster than the e1 → e() → e2 relaxation pathway; Figure 9). The simple carrier hypothesis, therefore, predicts that S1 will increase the amount of e(S) but not the rate of e(S) formation. The tetramer model predicts that the amount of e(S) formed is independent of S1 but that the rate of formation is increased by S1 because of allosteric interactions between the subunits. In two exploratory experiments measuring the uptake of 50 μM 3MG in intact cells, we observe that 1 mM unlabeled intracellular 3MG increases C_{rapid} from 0.031 ± 0.009 to 0.060 ± 0.013, while k_{rapid} is unchanged (68 ± 11 s^{-1}). This suggests that the former rather than the latter model may be more consistent with the data. k_{fast} was also increased from 0.043 ± 0.004 to 0.100 ± 0.008 s^{-1} by $3MG_i$. This result is expected for simple competitive inhibition of a binding process ($k_{obs} = k_{off} + k_{on}([3MG_i] + [^{14}C\text{-}3MG_i]$) and is consistent with the hypothesis that imported radiolabeled extracellular sugar and unlabeled intracellular sugar compete for binding at a GluT1 cytoplasmic site. More detailed analyses must be performed to confirm these findings and to examine the effects of intracellular ATP on these processes.

Compartment Sizes. Most of the experiments reported in the present study were carried out at [3MG] = 50 μM. It is useful to consider the compartment sizes that would result if the proposed transport mechanism were correct. The starting assumptions are as follows: (1) the free water space of a red cell is 60 fL (*11*); (2) the GluT1 content of a red cell is 600 000 copies per cell (*27*); (3) $K_{d(app)}$ for 3MG binding to e2 is 340 μM (Figure 7B); (4) the number of ATP-dependent, noncatalytic 3MG-binding sites in the "cage" is *n*; and (5) $K_{d(app)}$ for 3MG binding to these noncatalytic sites is extremely low, and the sites are always occupied (1 molecule in the LacY e1 cavity [1.5×10^{-24} L (*12*, *18*)] would produce a [3MG] of 1.1 M). With these starting assumptions, the relative amounts of cellular 3MG in the forms of e(S) (rapid compartment), eS_{cage} (fast compartment), and cell water (slow compartment) at equilibrium are 3.5:24.1:72.4 (when $n = 1$), 2.8:38.9:58.3 (when $n = 2$), and 2.3:48.8:48.8 (when $n = 3$). These numbers are generally consistent with the available data and suggest that *n* lies between 2 and 3. The LacY e1 cavity is large enough to hold as many as 3−5 hydrated glucose molecules (*12*). The slow rate of loss of sugar from the cage to cytosol may reflect the very significant probability of reassociation of sugar in the cage with the noncatalytic binding sites. As [3MG] is increased, the relative contribution of C_{rapid} and C_{fast} to the total cellular 3MG space should fall significantly. This has been observed previously (*11*).

CONCLUSIONS

The present study demonstrates that the time course of 3MG uptake at 4−22 °C by human RBCs is comprised of three sequential phases: rapid, fast, and slow. Each phase is inhibited by inhibitors of carrier-mediated glucose transport. The rapid phase is more strongly temperature-dependent than the fast and slow phases. The rapid phase does not represent the reaction between the sugar and carrier to form a carrier−sugar complex. Rather, it may represent the subsequent conversion of the carrier−substrate complex to an intermediate form [e(S)], in which the bound sugar is occluded within the translocation pathway. This occluded form of carrier can be isolated (with 10% efficiency) in the presence of transport inhibitors, which render the occluded sugar inaccessible to interstitium and cytosol.

REFERENCES

1. Joost, H. G., Bell, G. I., Best, J. D., Birnbaum, M. J., Charron, M. J., Chen, Y. T., Doege, H., James, D. E., Lodish, H. F., Moley, K. H., Moley, J. F., Mueckler, M., Rogers, S., Schurmann, A., Seino, S., and Thorens, B. (2002) Nomenclature of the GLUT/SLC2A family of sugar/polyol transport facilitators, *Am. J. Physiol. Endocrinol. Metab. 282*, E974−E976.
2. Widdas, W. F. (1952) Inability of diffusion to account for placental glucose transfer in the sheep and consideration of the kinetics of a possible carrier transfer, *J. Physiol. 118*, 23−39.
3. Stein, W. D. (1986) *Transport and Diffusion Across Cell Membranes*, Academic Press, New York.
4. Appleman, J. R., and Lienhard, G. E. (1985) Rapid kinetics of the glucose transporter from human erythrocytes. Detection and measurement of a half-turnover of the purified transporter, *J. Biol. Chem. 260*, 4575−4578.
5. Lowe, A. G., and Walmsley, A. R. (1986) The kinetics of glucose transport in human red blood cells, *Biochim. Biophys. Acta 857*, 146−154.
6. Naftalin, R. J., and Holman, G. D. (1977) Transport of sugars in human red cells, in *Membrane Transport in Red Cells* (Ellory, J. C., and Lew, V. L., Eds.) pp 257−300, Academic Press, New York.
7. Helgerson, A. L., and Carruthers, A. (1987) Equilibrium ligand binding to the human erythrocyte sugar transporter. Evidence for two sugar-binding sites per carrier, *J. Biol. Chem. 262*, 5464−5475.
8. Carruthers, A., and Zottola, R. J. (1996) Erythrocyte sugar transport, in *Handbook of Biological Physics. Transport Processes in Eukaryotic and Prokaryotic Organisms* (Konings, W. N., and L., H. R. K. J. S., Eds.) pp 311−342, Elsevier, The Netherlands.
9. Hebert, D. N., and Carruthers, A. (1992) Glucose transporter oligomeric structure determines transporter function. Reversible redox-dependent interconversions of tetrameric and dimeric GLUT1, *J. Biol. Chem. 267*, 23829−23838.
10. Naftalin, R. J., Smith, P. M., and Roselaar, S. E. (1985) Evidence for non-uniform distribution of D-glucose within human red cells during net exit and counterflow, *Biochim. Biophys. Acta 820*, 235−249.

11. Cloherty, E. K., Sultzman, L. A., Zottola, R. J., and Carruthers, A. (1995) Net sugar transport is a multi-step process. Evidence for cytosolic sugar binding sites in erythrocytes, *Biochemistry 34*, 15395−15406.
12. Abramson, J., Smirnova, I., Kasho, V., Verner, G., Kaback, H. R., and Iwata, S. (2003) Structure and mechanism of the lactose permease of *Escherichia coli*, *Science 301*, 610−615.
13. Kaback, H. R., Voss, J., and Wu, J. (1997) Helix packing in polytopic membrane proteins: Ihe lactose permease of *Escherichia coli*, *Curr. Opin. Struct. Biol. 7*, 537−542.
14. Pao, S. S., Paulsen, I. T., and Saier, M. H., Jr. (1998) Major facilitator superfamily, *Microbiol. Mol. Biol. Rev. 62*, 1−34.
15. Joost, H. G., and Thorens, B. (2001) The extended GLUT-family of sugar/polyol transport facilitators: Nomenclature, sequence characteristics, and potential function of its novel members (review), *Mol. Membr. Biol. 18*, 247−256.
16. Baker, P. F., and Carruthers, A. (1981) Sugar transport in giant axons of loligo, *J. Physiol. 316*, 481−502.
17. Lemieux, M. J., Song, J., Kim, M. J., Huang, Y., Villa, A., Auer, M., Li, X. D., and Wang, D. N. (2003) Three-dimensional crystallization of the *Escherichia coli* glycerol-3-phosphate transporter: A member of the major facilitator superfamily, *Protein Sci. 12*, 2748−2756.
18. Huang, Y., Lemieux, M. J., Song, J., Auer, M., and Wang, D. N. (2003) Structure and mechanism of the glycerol-3-phosphate transporter from *Escherichia coli*, *Science 301*, 616−620.
19. Baker, G. F., and Naftalin, R. J. (1979) Evidence of multiple operational affinities for D-glucose inside the human erythrocyte membrane, *Biochim. Biophys. Acta 550*, 474−484.
20. Cloherty, E. K., Heard, K. S., and Carruthers, A. (1996) Human erythrocyte sugar transport is incompatible with available carrier models, *Biochemistry 35*, 10411−10421.
21. Lieb, W. R., and Stein, W. D. (1974) Testing and characterizing the simple carrier, *Biochim. Biophys. Acta 373*, 178−196.
22. Ginsburg, H., and Stein, D. (1975) Zero-trans and infinite-cis uptake of galactose in human erythrocytes, *Biochim. Biophys. Acta 382*, 353−368.
23. Karlish, S. J. D., Lieb, W. R., Ram, D., and Stein, W. D. (1972) Kinetic parameters of glucose efflux from human red blood cells under zero-trans conditions, *Biochim. Biophys. Acta 255*, 126−132.
24. Miller, D. M. (1968) The kinetics of selective biological transport. III. Erythrocyte-monosaccharide transport data, *Biophys. J. 8*, 1329−1338.
25. Hebert, D. N., and Carruthers, A. (1991) Uniporters and anion antiporters. *Curr. Opin. Cell Biol. 3*, 702−709.
26. Levine, K. B., Cloherty, E. K., Hamill, S., and Carruthers, A. (2002) Molecular determinants of sugar transport regulation by ATP, *Biochemistry 41*, 12629−12638.
27. Heard, K. S., Fidyk, N., and Carruthers, A. (2000) ATP-dependent substrate occlusion by the human erythrocyte sugar transporter, *Biochemistry 39*, 3005−3014.
28. Blodgett, D. M., and Carruthers, A. (2004) Conventional transport assays underestimate sugar transport rates in human red cells, *Blood Cells, Mol. Dis. 32*, 401−407.
29. Gutfreund, H. (1969) Rapid mixing: Continuous flow, *Methods Enzymol. 16*, 229−249.
30. Coderre, P. E., Cloherty, E. K., Zottola, R. J., and Carruthers, A. (1995) Rapid substrate translocation by the multi-subunit, erythroid glucose transporter requires subunit associations but not cooperative ligand binding, *Biochemistry 34*, 9762−9773.
31. Levine, K. B., Cloherty, E. K., Fidyk, N. J., and Carruthers, A. (1998) Structural and physiologic determinants of human erythrocyte sugar transport regulation by adenosine triphosphate, *Biochemistry 37*, 12221−12232.
32. Carruthers, A., and Helgerson, A. L. (1991) Inhibitions of sugar transport produced by ligands binding at opposite sides of the membrane. Evidence for simultaneous occupation of the carrier by maltose and cytochalasin B, *Biochemistry 30*, 3907−3915.
33. Hamill, S., Cloherty, E. K., and Carruthers, A. (1999) The human erythrocyte sugar transporter presents two sugar import sites, *Biochemistry 38*, 16974−16983.
34. Lieb, W. R., and Stein, W. D. (1986) in *Transport and Diffusion Across Cell Membranes*, pp 69−112, Academic Press, New York.
35. Carruthers, A. (1986) ATP regulation of the human red cell sugar transporter, *J. Biol. Chem. 261*, 11028−11037.
36. Mercer, R. W., and Dunham, P. B. (1981) Membrane-bound ATP fuels the Na/K pump. Studies on membrane-bound glycolytic enzymes on inside-out vesicles from human red cell membranes, *J. Gen. Physiol. 78*, 547−568.
37. Singh, R., Barden, A., Mori, T., and Beilin, L. (2001) Advanced glycation end-products: A review, *Diabetologia 44*, 129−146.
38. Carruthers, A., and Melchior, D. L. (1985) Transport of α- and β-D-glucose by the intact human red cell, *Biochemistry 24*, 4244−4250.
39. Pessino, A., Hebert, D. N., Woon, C. W., Harrison, S. A., Clancy, B. M., Buxton, J. M., Carruthers, A., and Czech, M. P. (1991) Evidence that functional erythrocyte-type glucose transporters are oligomers, *J. Biol. Chem. 266*, 20213−20217.
40. Masaik, S. J., and LeFevre, P. G. (1977) Glucose transport inhibition by proteolytic degradation of the human erythrocyte membrane inner surface, *Biochim. Biophys. Acta 465*, 371−377.
41. Naftalin, R. J., and Arain, M. (1999) Interactions of sodium pentobarbital with D-glucose and L-sorbose transport in human red cells, *Biochim. Biophys. Acta 1419*, 78−88.
42. Afzal, I., Cunningham, P., and Naftalin, R. J. (2002) Interactions of ATP, oestradiol, genistein, and the anti-oestrogens, faslodex (ICI 182780) and tamoxifen, with the human erythrocyte glucose transporter, GLUT1, *Biochem. J. 365*, 707−719.
43. Baldwin, S. A., Baldwin, J. M., Gorga, F. R., and Lienhard, G. E. (1979) Purification of the cytochalasin B binding component of the human erythrocyte monosaccharide transport system, *Biochim. Biophys. Acta 552*, 183−188.
44. Sultzman, L. A., and Carruthers, A. (1999) Stop-flow analysis of cooperative interactions between GLUT1 sugar import and export sites, *Biochemistry 38*, 6640−6650.
45. Appleman, J. R., and Lienhard, G. E. (1989) Kinetics of the purified glucose transporter. Direct measurement of the rates of interconversion of transporter conformers, *Biochemistry 28*, 8221−8227.
46. Connolly, T. J., Carruthers, A., and Melchior, D. L. (1985) Effects of bilayer cholesterol on human erythrocyte hexose transport protein activity in synthetic lecithin bilayers, *Biochemistry 24*, 2865−2873.
47. Connolly, T. J., Carruthers, A., and Melchior, D. L. (1985) Effect of bilayer cholesterol content on reconstituted human erythrocyte sugar transporter activity, *J. Biol. Chem. 260*, 2617−2620.
48. Carruthers, A., and Melchior, D. L. (1984) Human erythrocyte hexose transporter activity is governed by bilayer lipid composition in reconstituted vesicles, *Biochemistry 23*, 6901−6911.
49. Glynn, I. M., Hara, Y., and Richards, D. E. (1984) The occlusion of sodium ions within the mammalian sodium−potassium pump: Its role in sodium transport, *J. Physiol. 351*, 531−547.
50. Glynn, I. M., and Richards, D. E. (1982) Occlusion of rubidium ions by the sodium−potassium pump: Its implications for the mechanism of potassium transport, *J. Physiol. 330*, 17−43.
51. Salas-Burgos, A., Iserovich, P., Zuniga, F., Vera, J. C., and Fischbarg, J. (2004) Predicting the three-dimensional structure of the human facilitative glucose transporter glut1 by a novel evolutionary homology strategy: Insights on the molecular mechanism of substrate migration, and binding sites for glucose and inhibitory molecules, *Biophys. J. 87*, 2990−2999.

BI048247M